Pergamon

Geochimica et Cosmochimica Acta, Vol. 67, No. 3, pp. 345–360, 2003

0016-7037/03 $22.00 + .00

PII S0016-7037(02)01115-8

Laboratory determination of thermal diffusion constants for $^{29}N_2/^{28}N_2$ in air at temperatures from −60 to 0°C for reconstruction of magnitudes of abrupt climate changes using the ice core fossil–air paleothermometer

ALEXI M. GRACHEV* and JEFFREY P. SEVERINGHAUS

Geosciences Research Division, Scripps Institution of Oceanography, 9500 Gilman Dr., La Jolla, CA 92093-0244, USA

(*Received February* 27, 2002; *accepted in revised form July* 30, 2002)

Abstract—Rapid temperature change causes fractionation of isotopic gaseous species in air in firn (snow) by thermal diffusion, producing a signal that is preserved in trapped air bubbles as the snow forms ice. Using a model of heat penetration and gas diffusion in the firn, as well as the values of appropriate thermal diffusion constants, it is possible to reconstruct the magnitude of a particular paleoclimate change. Isotopic nitrogen in air serves as a convenient tracer for such paleoreconstruction, because the ratio $^{29}N_2/^{28}N_2$ has stayed extremely constant in the atmosphere for $\geq 10^6$ years. However, prior to this work no data were available for thermal diffusion of $^{29}N_2/^{28}N_2$ in air, but only in pure N_2. We devised a laboratory experiment allowing fractionation of gases by thermal diffusion in a small, tightly controlled temperature difference. A mass spectrometer was employed in measuring the resulting fractionations yielding measurement precision greater than was attainable by earlier thermal diffusion investigators.

Our laboratory experiments indicate that the value of the thermal diffusion sensitivity (Ω) for $^{29}N_2/^{28}N_2$ in air is $+(14.7 \pm 0.5) \times 10^{-3}$ per mil/°C when the average temperature is –30.0°C. The corresponding value for $^{29}N_2/^{28}N_2$ in pure N_2 that we find is $+(15.3 \pm 0.4) \times 10^{-3}$ per mil/°C at –30.6°C, in agreement with the previously available literature data within their large range of uncertainty. We find that an empirical equation, $\Omega = (8.656/T_K - 1232/T_K^2) \pm 3\%$ per mil/°C, describes the slight variation of the sensitivity values for $^{29}N_2/^{28}N_2$ in air with temperature in the range of −60 to 0°C. A separate set of experiments also described in this paper rules out adsorption as a candidate for producing additional temperature change-driven fractionation of $^{29}N_2/^{28}N_2$ in the firn air. The combined newly obtained data constitute a calibration of the fossil–air paleothermometer with respect to isotopic nitrogen and will serve to improve the estimates of the magnitudes of past abrupt climate changes recorded in ice cores.

1. INTRODUCTION

A new method has been developed recently to allow precise reconstruction of the magnitudes of abrupt climate changes using fossil air from ice cores (Severinghaus et al., 1998; Severinghaus and Brook, 1999; Leuenberger et al., 1999; Lang et al., 1999; Jouzel, 1999; Caillon et al., 2001). The method is based on the physics of air diffusion at the top of ice sheets in the ~100-m deep layer of consolidated snow called "firn." Firn is a porous medium that is very effective in suppressing convective movement of gas, making molecular diffusion the dominant transport mechanism. Fossil air preserved in bubbles in ice cores was at one time freely-diffusing air just above the firn–ice transition. Air becomes trapped when the lowermost portion of the firn is gradually metamorphosed into ice under the ever-increasing weight of the newly deposited snow at the surface. Fast shifts of surface temperature are capable of making the firn column nonisothermal (due to its lower portion being more insulated) for prolonged periods of time, which in turn causes a change in isotopic composition of air at the bottom of the firn through the action of a subtle physical phenomenon known as "thermal diffusion." The validity of the fossil air paleothermometer has been tested in the modern polar firn as described by Severinghaus et al. (2001). An example of an observed isotopic profile of nitrogen and argon in the Greenland Ice Sheet Project 2 (GISP2) ice core is shown in Figure 1. Once the appropriate values of thermal diffusion constants are known, the method allows an unambiguous estimate of the magnitude of the abrupt climate warmings and coolings that occurred persistently in Greenland (and elsewhere) throughout the Last Glacial Period (Alley et al., 2001; Blunier and Brook, 2001). This was not possible with previously available methods (see Jouzel, 2001).

1.1. The Thermal Diffusion Phenomenon

The process of thermal diffusion (Chapman, 1917; Enskog, 1917; Chapman and Dootson, 1917) can be defined as the tendency of initially uniform mixtures to unmix (fractionate locally) when subjected to nonuniform temperature conditions. This phenomenon is unrelated to the simple fact that there are more molecules overall at lower than at higher temperatures, pressure being equal. In the case of thermal diffusion the diffusive mass transport is driven by a thermal gradient rather than by a concentration gradient as in the case of ordinary diffusion. The case of thermal diffusion is distinctly different from the other three transport properties (viscosity, thermal conductivity, and ordinary diffusion) in that a gradient of one quantity (temperature) results in a transport of an unrelated quantity (mass). This subtle phenomenon can be derived theoretically using the methods of the rigorous kinetic theory of gases (Hirschfelder et al., 1964; Mason et al., 1966; Chapman and Cowling, 1970) or of nonequilibrium thermodynamics (De

* Author to whom correspondence should be addressed (agrachev@ucsd.edu).

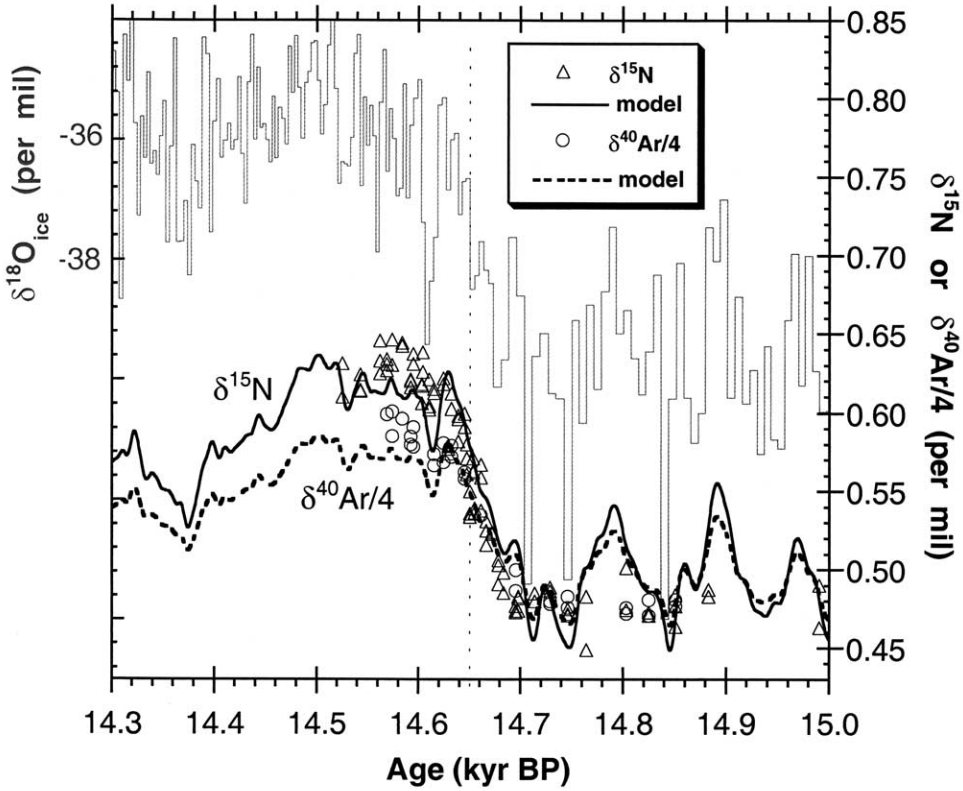

Fig. 1. A profile of $\delta^{15}N^{(*)}$ and $\delta^{40}Ar$ in fossil air extracted from a ~15,000-year-old section of GISP2 ice core. The observed isotopic anomaly in conjunction with a model of heat penetration and diffusion in the firn allows an estimate of the magnitude of the warming (~11°C in the case of the "Bølling warming" shown in the figure; see Severinghaus and Brook, 1999 and Severinghaus et al., 2003). Thermal diffusion sensitivity values in air from this work served as input parameters of the model. The conventional paleotemperature proxy $\delta^{18}O_{ice}$ is shown as a reference. (*) $\delta^{15}N \equiv \{[(^{29}N_2/^{28}N_2)_{sample}/(^{29}N_2/^{28}N_2)_{standard}] - 1]\} \times 1{,}000$ per mil; similar definition applies to the $^{40}Ar/^{36}Ar$ ratio ($\delta^{40}Ar$). The values of $\delta^{40}Ar$ are scaled by a factor of 1/4 in order to display the delta values per unit mass difference in respective isotopic species. The offset between the profiles of $\delta^{15}N$ and $\delta^{40}Ar/4$ is due to their different thermal diffusion sensitivity values.

Groot, 1959). The simple ("Maxwellian") gas kinetic theory fails to account for it. Generally speaking, the greater the mass difference between the molecules of the two species in a mixture, and the "harder" the collisions between them (i.e., a steeper repulsive wall of the intermolecular potential), the greater is the tendency of the two species to separate by thermal diffusion.

The thermal diffusion process can be observed in a laboratory in a vertically mounted closed tube containing a uniform mixture of gases or isotopic species by heating it from above and chilling it from below, and detecting the subsequent slight change of composition at its cold end relative to its warm end. Unmixing driven by thermal diffusion can only proceed up to a certain point: the increased mole fraction gradient enables ordinary diffusion to support an equal and opposite flux of respective molecules balancing the flux due to thermal diffusion. The corresponding steady-state fractionation increases with the imposed temperature difference. The effect is linear in the sense that a doubling of the imposed temperature difference results in a doubling of fractionation within temperature differences of ~100°C. For the majority of studied mixtures, the heavier component migrates down the temperature gradient, and the lighter component up. A number of excellent reviews on the complex phenomenon of gaseous thermal diffusion are available, most notably Grew and Ibbs (1952), Mason et al. (1966), and Grew (1969).

Although many attempts have been made to offer a simple explanation of thermal diffusion (see references in Cowling, 1970), none of the explanations proved completely satisfactory (Mason et al., 1966; Monchick and Mason, 1967; Grew, 1969). Still, we can make the most basic point regarding the driving force of the unmixing by thermal diffusion, as follows. The two components in a binary mixture are "pushed apart" by thermal diffusion. Opposing partial pressure gradients are established for each of them as a result. (The total pressure is the same throughout the vessel because the mixture is not flowing as a whole). Focusing on one component, a force has to be constantly applied to it to maintain its partial pressure gradient. It is easy to recognize that such a force must originate from the second component. The mechanism of generating the force lies in the exchange of momentum between the components in collisions (from Newton's law a force is equivalent to the rate of change of momentum). In a mixture subjected to a temperature difference there is a constant net transfer of momentum

from one component to the other, hence the force that "pushes" them apart. Attempts to take this momentum transfer argument further to match the result of the rigorous theory (Frankel, 1940; Jones and Furry, 1946; Furry, 1948; Present, 1958) have been criticized as being inadequate and ad hoc (Mason et al., 1966; Monchick and Mason, 1967). Rigorous theory supplies mathematical derivation of thermal diffusion but unfortunately no intuitive explanation of it (see however Cowling, 1970 for an elementary interpretation of the exact theory).

1.2. The Thermal Diffusion Constants

The rigorous kinetic theory yields the following expressions for the fluxes of gases in a nonuniform binary mixture in a temperature gradient:

$$\boldsymbol{J_1} = -nD_{12}(\,grad X_1 + \alpha_T X_1 X_2\, grad(\ln T)), \qquad (1a)$$

$$\boldsymbol{J_2} = -nD_{12}(\,grad X_2 - \alpha_T X_1 X_2 grad(\ln T)), \qquad (1b)$$

where $\boldsymbol{J_1}$ and $\boldsymbol{J_2}$ are the vectors of flux densities (molecules/cm^2-s) of species *1* and *2* ($\boldsymbol{J_1} + \boldsymbol{J_2} = 0$), n is the total number density of molecules (molecules/cm^3), X_1 and X_2 are mole fractions of the components ($X_1 + X_2 = 1$), D_{12} is the ordinary diffusion coefficient, T is temperature (in Kelvin), and α_T is the so-called "thermal diffusion factor" (Grew and Ibbs, 1952; Chapman and Cowling, 1970; Mason et al., 1966; Grew, 1969). By convention, gas *1* is the heavier component of the mixture so that when $\alpha_T > 0$ (the most common case) the heavier component moves down the temperature gradient, and the lighter component in the opposite direction.

The values of α_T vary substantially from mixture to mixture, and depend on the absolute temperature (Mason et al., 1966). There is also an effect of composition and of pressure on thermal diffusion, the latter becoming particularly pronounced at pressures greatly exceeding 1 atm (Mason et al., 1966; Velds et al., 1967; Oost, 1968; Oost et al., 1972; also see Dunlop and Bignell, 1996 and references therein). Because the accuracy of theoretical calculations of the thermal diffusion factors still needs improvement, especially for multicomponent mixtures (Hirschfelder et al., 1964; Kestin et al., 1984; Boushehri et al., 1987; Kincaid et al., 1987; Bzowski et al., 1990), experimental methods have been used widely to determine their values. Experimental determination of thermal diffusion factors has most commonly employed a so-called "two-bulb apparatus," which consists of two large volumes, one above the other, connected by a narrow tube (Mason et al., 1966). A cascade device called a trennschaukel (or swing separator) has also been successfully employed for that purpose. The use of a more complex apparatus called a "thermal diffusion column" can only yield approximate α_T values when empirical "apparatus factors" are estimated from calibration experiments (Mason et al., 1966). A large dataset on thermal diffusion factors for various pure binary mixtures is available in the literature (see references in Grew and Ibbs, 1952 and Mason et al., 1966).

The thermal diffusion factor is determined from an experiment using a two-bulb apparatus as follows. The upper volume ("bulb") is kept at a temperature T_{hot} and the lower volume at a temperature T_{cold}. The vertical mounting of the apparatus with the warmer bulb above obviates convective currents. A steady state is approached exponentially with the relaxation time τ, which is determined mainly by the dimensions of the apparatus and the ordinary diffusion coefficient D_{12} for the mixture (Grew and Ibbs, 1952; Mason et al., 1966 and references therein). In the steady state, fluxes $\boldsymbol{J_1}$ and $\boldsymbol{J_2}$ of Eqns. 1a and 1b become equal to zero. Denoting the vertical axis as z, the steady-state form of Eqn. 1a can be written as:

$$dX_1/dz = -\alpha_T X_1 X_2\, d(\ln T)/dz. \qquad (2)$$

Equation 2 can be integrated with the assumption of uniform composition in each bulb and taking the temperature-dependent parameter α_T to correspond to some intermediate temperature between T_{cold} and T_{hot} denoted as the effective average temperature, $T_{av.}$:

$$\ln[(X_{1cold}/X_{2cold})/(X_{1hot}/X_{2hot})] = \alpha_T(T_{av.}) \times \ln(T_{hot}/T_{cold}). \qquad (3)$$

This equation (Grew and Ibbs, 1952; Mason et al., 1966) relates the steady-state mole fractions of the components in the two bulbs to the temperatures T_{hot} and T_{cold} (in degrees Kelvin) at which they are maintained in an experiment. The actual value of the average temperature $T_{av.}$ can be found once a certain algebraic form of the temperature dependence of the thermal diffusion factor is assumed. If this dependence is taken to be of the widely used form $\alpha_T \approx a - b/T_K$ (Brown, 1940; Grew and Ibbs, 1952), where a and b are arbitrary constants, then the effective average temperature is given as (Mason et al., 1966):

$$T_{av.} = ((T_{hot}T_{cold})/(T_{hot} - T_{cold})) \times \ln(T_{hot}/T_{cold}), \qquad (4)$$

where all temperatures are expressed in degrees Kelvin. The quantity in square brackets in Eqn. 3 is called the "separation factor" (Grew and Ibbs, 1952) and is denoted as q in the literature:

$$q \equiv (X_{1\,cold}/X_{2\,cold})/(X_{1\,hot}/X_{2\,hot}). \qquad (5)$$

Temperatures T_{hot} and T_{cold} are chosen by the experimenter, and the quantity q can be determined by analyzing the steady-state composition of the mixture sampled from the hot and cold bulbs using mass spectrometry or other analytical techniques (Mason et al., 1966).

While the thermal diffusion factor is a parameter conventionally used in the physics literature, a new measure of susceptibility of isotopic species to unmixing by thermal diffusion has been introduced recently called the "thermal diffusion sensitivity" Ω (Severinghaus et al., 2001; Severinghaus et al., 2003). It is defined in terms of easily identifiable quantities and its form resembles customary geochemical and paleoclimatological indicators. The starting point in the definition is to express the relative fractionation of the two isotopic species due to thermal diffusion using delta notation:

$$\delta^* = (q - 1) \times 1{,}000 \text{ per mil}. \qquad (6)$$

The asterisk is used as a reminder that no standard is used when determining the fractionation, but rather the isotopic ratio in the cold bulb of the apparatus is measured relative to the ratio in the hot bulb (refer to Eqn. 5). The thermal diffusion sensitivity is then given as:

$$\Omega(T_{av.}) \equiv \delta^*/(T_{hot} - T_{cold}) \text{ per mil/°C.} \quad (7)$$

The sensitivity is referenced to the average temperature $T_{av.}$ given by Eqn. 4 in an analogous way as the thermal diffusion factor of Eqn. 3. Note that while the thermal diffusion factor is a pure number, the sensitivity has units of per mil/°C. This parameter bears a straightforward meaning: it shows by how much two isotopic species in a mixture fractionate (in steady state) for each degree of applied temperature difference. The value of the thermal diffusion sensitivity is readily calculated from an experiment using Eqn. 7. Combining Eqns. 3, 5, and 6 and using the same δ^* notation, the thermal diffusion factor corresponding to the effective average temperature $T_{av.}$ of Eqn. 4 is calculated as:

$$\alpha_T(T_{av.}) = \ln(1 + 0.001 \times \delta^*)/\ln(T_{hot}/T_{cold}). \quad (8)$$

The approximate relationship between $\Omega(T_{av.})$ and $\alpha_T(T_{av.})$ is given as follows:

$$\Omega(T_{av.}) \approx \alpha_T(T_{av.}) \times 1000/T_{av.} \text{ per mil/°C,} \quad (9)$$

where the effective average temperature $T_{av.}$ is in degrees Kelvin (see Appendix). This approximation is very accurate for small temperature differences.

1.3. The Objective of This Work

Our interest in thermal diffusion lies in its role in generating a record of abrupt climate changes preserved in archives of fossil air from ice cores. Previous work has employed the stable isotopic species of either isotopic nitrogen $^{29}N_2/^{28}N_2$ alone (Leuenberger et al., 1999; Lang et al., 1999) or a combination of isotopic nitrogen and isotopic argon $^{40}Ar/^{36}Ar$ (Severinghaus et al., 1998; Severinghaus and Brook, 1999; Caillon et al., 2001) for the purpose of establishing the degree to which the fossil air extracted from ice cores is fractionated by thermal diffusion. Knowledge of the thermal diffusion constants of the above isotopic species for appropriate conditions is critical in recovering the magnitudes of abrupt climate shifts from the amounts of observed thermal diffusion fractionation.

Unfortunately the literature supplies no data on thermal diffusion of isotopic nitrogen and argon in air, but only in pure respective gases (Stier, 1942; Mann, 1948; Davenport and Winter, 1951; Moran and Watson, 1958; Saxena et al., 1961; Paul et al., 1963; Boersma-Klein and De Vries, 1966; Raman et al., 1968; Stevens and De Vries, 1968; Rutherford, 1973; Taylor and Weissman, 1973; Santamaria et al., 1977). The distinction is important to make in view of the fact that isotopic pairs in pure and in mixed gases can have rather different thermal diffusion factors (Van der Valk and De Vries, 1963; Kincaid et al., 1987). Although one may expect the difference to be more pronounced for argon (~1% in air) than for nitrogen (~78% in air) due to greater dilution of the argon gas, it is not clear a priori how close the pure gas thermal diffusion constants are to the respective constants in air in either case.

We have developed a laboratory procedure allowing precise determination of thermal diffusion constants of isotopic N_2 and Ar in air. Our technique is conceptually similar to that employed by earlier workers (see Section 2.1). However, we used a smaller size of fractionation apparatus, thus making experiment durations relatively short. We also avoided the use of multistage isotopic enrichment procedures, thus reducing the potential for systematic error. We used small temperature differences representative of climate, i.e., ~15°C, and hence were capable of more accurate temperature assignment of α_T values, while still being able to detect resulting small fractionations with high precision. These improvements were made possible by having firm temperature control during experiments and by employing a modern dual-inlet mass spectrometer of much higher sensitivity and precision than instruments available to the pioneers of thermal diffusion studies.

This study presents the results of our thermal diffusion experiments on $^{29}N_2/^{28}N_2$ in air and in pure nitrogen. In addition, we present results of a separate experimental investigation of possible temperature change–driven fractionation effects related to surface adsorption in the firn. The overall goal of this work was to establish an accurate calibration for the recently developed ice core fossil–air paleothermometer.

2. EXPERIMENTAL METHODS

2.1. Thermal Diffusion Experiments

Dry air, water-saturated air, or N_2 was equilibrated in a firmly controlled temperature difference (or in an isothermal bath for "blank" experiments) using a two-bulb apparatus (see Section 1.2). The portion of air at the colder temperature became isotopically fractionated relative to the portion at the warmer temperature by thermal diffusion. The two were isolated from each other by closing off the appropriate valves once enough time had been allowed to reach a steady state. The amount of induced fractionation was measured on a mass spectrometer. For brevity we refer to the bringing of a mixture to a steady state with respect to thermal diffusion as "equilibration," while of course strictly speaking the situation is inherently a nonequilibrium one (a temperature difference is maintained and the composition of the mixture is nonuniform). The experiments performed during 1998–99 are referred to as the "early" experiments, whereas those for the time period 2000–02 are referred to as the "recent" experiments (Table 1a). The latter were characterized by somewhat more careful experimentation, and the corresponding data may be of slightly better quality.

2.1.1. Equilibration vessels

Two stainless steel equilibration vessels (hereafter the "small cell" and the "big cell") were employed in our experiments. The big cell is shown in Fig. 2 under label "1." The small cell had tube segments (of the same diameter as the middle tube) in place of the bulbs, but had otherwise the same geometry as the big cell. The total distance between the ends of a cell was ~32 cm and the inside cross section of the middle tube was ~0.34 cm^2. The bulb volume was ~26 cm^3 for the big cell and ~1.2 cm^3 for the small cell.

A cell was mounted vertically in a specially designed dual-temperature bath (see Section 2.1.4). The upper side of a cell is referred to as the "warm" side, and the lower as the "cold" side (see Fig. 2). Each side was equipped with a pair of valves. The inner valves served to isolate the two portions of fractionated gas from each other once the equilibration has been completed. The outer valves allowed the introduction of the gas into the mass spectrometer for the analysis. The end tubes curved at 90° were intended for connecting the cell to the mass spectrometer.

Originally the big cell was intended for experiments with argon, as more air was needed to perform the argon analysis. We later decided to use the big cell for the nitrogen experiments as well to test whether there is a contribution to the overall fractionation caused by surface effects (i.e., temperature-dependent isotope-selective adsorption on the stainless steel surface). Such effect should depend on the surface to volume ratio in the sample volume, which differed considerably for the two cells: it constituted roughly 15 cm^{-1} for the small cell and ~2 cm^{-1} for the big cell.

Table 1a. A complete list of the measured and derived parameters for the thermal diffusion experiments.

AIR-I: small cell/air/early data

T_{cold}[a]	T_{hot}	$\delta^*_{corr.}$	$T_{av.}$	$\alpha_T \times 10^3$	$\Omega \times 10^3$
−64.8	−50.4	0.209	−57.8	3.12	14.5
−64.7	−49.8	0.208	−57.4	3.01	13.9
−51.0	−36.7	0.205	−44.0	3.28	14.3
−51.0	−36.5	0.211	−43.9	3.34	14.6
−50.0	−35.2	0.225	−42.8	3.50	15.2
−50.1	−35.0	0.230	−42.7	3.51	15.2
−50.0	−34.7	0.213	−42.5	3.21	13.9
−50.0	−34.7	0.227	−42.5	3.43	14.8
−46.1	−36.7	0.129	−41.5	3.18	13.7
−46.1	−36.6	0.135	−41.4	3.28	14.2
−46.0	−36.6	0.130	−41.4	3.21	13.8
−35.5	−19.7	0.236	−27.8	3.67	15.0
−34.8	−20.4	0.222	−27.7	3.78	15.4
−35.4	−19.7	0.228	−27.7	3.56	14.5
−35.5	−19.5	0.239	−27.7	3.67	14.9
−35.3	−19.6	0.247	−27.6	3.86	15.7
−35.3	−19.4	0.230	−27.5	3.55	14.5
−34.6	−20.1	0.208	−27.5	3.52	14.3
−20.7	−5.2	0.228	−13.1	3.82	14.7
−20.5	−5.2	0.237	−13.0	4.03	15.5
−19.8	−5.5	0.210	−12.8	3.83	14.7
−19.8	−5.3	0.213	−12.7	3.82	14.7
−19.7	−5.0	0.230	−12.5	4.08	15.7
−19.7	−4.9	0.230	−12.4	4.05	15.5
−19.6	−5.0	0.217	−12.4	3.88	14.9
−19.6	−4.9	0.230	−12.4	4.09	15.7
−19.7	−4.7	0.219	−12.3	3.80	14.6
−5.4	9.1	0.234	1.7	4.44	16.1
−5.3	9.1	0.217	1.8	4.14	15.1
−5.3	9.2	0.214	1.8	4.06	14.8
−5.5	9.5	0.237	1.9	4.35	15.8

AIR-II: small cell/air/recent data

T_{cold}	T_{hot}	$\delta^*_{corr.}$	$T_{av.}$	$\alpha_T \times 10^3$	$\Omega \times 10^3$
−65.4	−50.5	0.211	−58.1	3.05	14.2
−65.4	−50.4	0.203	−58.1	2.91	13.5
−65.4	−50.3	0.205	−58.0	2.92	13.6
−65.3	−50.4	0.201	−58.0	2.90	13.5
−65.2	−50.4	0.209	−58.0	3.04	14.1
−65.1	−50.3	0.194	−57.9	2.82	13.1
−65.0	−50.2	0.201	−57.8	2.93	13.6
−65.0	−50.2	0.202	−57.8	2.94	13.6
−64.9	−50.2	0.197	−57.7	2.89	13.4
−49.9	−35.3	0.206	−42.8	3.25	14.1
−49.8	−35.1	0.216	−42.6	3.39	14.7
−38.5	−22.9	0.225	−30.9	3.50	14.4
−38.7	−22.6	0.236	−30.8	3.55	14.7
−38.6	−22.6	0.231	−30.8	3.50	14.4
−38.5	−22.6	0.234	−30.7	3.57	14.7
−38.3	−22.8	0.230	−30.7	3.60	14.8
−38.3	−22.8	0.227	−30.7	3.55	14.6
−37.8	−23.3	0.209	−30.7	3.50	14.4
−38.4	−22.6	0.232	−30.7	3.56	14.7
−37.7	−23.3	0.225	−30.6	3.79	15.6
−37.7	−23.3	0.211	−30.6	3.55	14.7
−38.3	−22.5	0.228	−30.6	3.50	14.4
−38.0	−22.8	0.231	−30.6	3.69	15.2
−37.5	−23.3	0.215	−30.5	3.67	15.1
−37.4	−23.4	0.215	−30.5	3.73	15.4
−37.5	−23.2	0.218	−30.5	3.70	15.2
−37.3	−23.4	0.205	−30.5	3.58	14.7
−37.3	−23.4	0.214	−30.5	3.74	15.4
−37.5	−23.1	0.224	−30.4	3.78	15.6

(continued)

Table 1a. (Continued)

AIR-II: small cell/air/recent data

T_{cold}[a]	T_{hot}	$\delta^*_{corr.}$	$T_{av.}$	$\alpha_T \times 10^3$	$\Omega \times 10^3$
−37.6	−22.5	0.210	−30.2	3.38	13.9
−37.6	−22.5	0.211	−30.2	3.40	14.0
−37.5	−22.5	0.209	−30.2	3.39	13.9

AIR-III: small cell/air+vapor/recent data

T_{cold}	T_{hot}	$\delta^*_{corr.}$	$T_{av.}$	$\alpha_T \times 10^3$	$\Omega \times 10^3$
−37.0	−22.2	0.222	−29.7	3.65	15.0
−36.9	−21.8	0.238	−29.5	3.84	15.8
−36.8	−21.6	0.223	−29.4	3.58	14.7
−36.7	−21.7	0.224	−29.4	3.64	14.9
−36.8	−21.4	0.228	−29.3	3.61	14.8
−36.7	−21.5	0.227	−29.3	3.64	14.9
−36.9	−21.2	0.234	−29.2	3.64	14.9
−36.7	−21.4	0.224	−29.2	3.57	14.6
−36.7	−21.4	0.218	−29.2	3.48	14.2

AIR-IV: big cell/air/early data (excluded)

T_{cold}	T_{hot}	$\delta^*_{corr.}$	$T_{av.}$	$\alpha_T \times 10^3$	$\Omega \times 10^3$
−35.4	−19.7	0.224	−27.7	3.51	14.3
−35.4	−19.5	0.220	−27.6	3.40	13.8
−35.2	−19.6	0.226	−27.6	3.56	14.5
−35.5	−19.0	0.247	−27.4	3.69	15.0
−35.2	−19.2	0.204	−27.4	3.13	12.7
−35.2	−17.4	0.248	−26.5	3.44	13.9

AIR-V: big cell/50 torr air/recent data

T_{cold}	T_{hot}	$\delta^*_{corr.}$	$T_{av.}$	$\alpha_T \times 10^3$	$\Omega \times 10^3$
−49.9	−35.3	0.208	−42.8	3.28	14.2
−38.3	−23.2	0.217	−30.9	3.48	14.4
−38.1	−23.1	0.208	−30.8	3.36	13.9
−37.9	−23.2	0.216	−30.7	3.56	14.7
−37.9	−23.2	0.215	−30.7	3.55	14.6
−37.7	−23.4	0.209	−30.7	3.54	14.6
−38.1	−22.9	0.215	−30.7	3.43	14.1
−38.0	−23.0	0.210	−30.7	3.40	14.0
−38.0	−23.0	0.216	−30.7	3.49	14.4
−37.6	−23.4	0.211	−30.6	3.60	14.9
−37.6	−23.4	0.219	−30.6	3.74	15.4
−37.8	−23.1	0.208	−30.6	3.43	14.1
−37.8	−23.1	0.215	−30.6	3.55	14.6
−37.6	−23.3	0.224	−30.6	3.80	15.7
−37.4	−23.5	0.207	−30.6	3.61	14.9
−37.5	−23.3	0.212	−30.5	3.62	14.9
−37.6	−23.1	0.220	−30.5	3.68	15.2
−37.5	−23.2	0.206	−30.5	3.50	14.4
−37.5	−23.2	0.220	−30.5	3.73	15.4
−37.6	−22.5	0.212	−30.2	3.41	14.0
−37.6	−22.2	0.209	−30.1	3.30	13.6

AIR-VI: big cell/air/recent data

T_{cold}	T_{hot}	$\delta^*_{corr.}$	$T_{av.}$	$\alpha_T \times 10^3$	$\Omega \times 10^3$
−38.1	−22.8	0.219	−30.6	3.47	14.3
−37.9	−22.9	0.221	−30.6	3.57	14.7
−37.9	−22.8	0.216	−30.5	3.47	14.3
−37.8	−22.6	0.221	−30.4	3.53	14.5
−37.7	−22.5	0.223	−30.3	3.56	14.7
−37.6	−22.6	0.215	−30.3	3.48	14.3

(continued)

Table 1a. (Continued)

AIR-VI: big cell/air/recent data

T_{cold}[a]	T_{hot}	$\delta^*_{corr.}$	$T_{av.}$	$\alpha_T \times 10^3$	$\Omega \times 10^3$
−37.6	−22.5	0.219	−30.2	3.52	14.5
−37.5	−22.6	0.217	−30.2	3.54	14.6
−37.4	−22.5	0.222	−30.1	3.62	14.9

N2-I: small cell/N_2/early data

T_{cold}	T_{hot}	$\delta^*_{corr.}$	$T_{av.}$	$\alpha_T \times 10^3$	$\Omega \times 10^3$
−35.4	−19.8	0.242	−27.8	3.80	15.5
−35.3	−19.8	0.235	−27.7	3.72	15.1
−35.3	−19.7	0.238	−27.7	3.74	15.2
−35.3	−19.6	0.230	−27.6	3.60	14.6
−35.3	−19.6	0.232	−27.6	3.62	14.7
−35.1	−19.6	0.224	−27.5	3.55	14.5
−35.1	−19.5	0.226	−27.5	3.57	14.5
−35.1	−19.5	0.234	−27.5	3.68	15.0

N2-II: small cell/N_2/recent data

T_{cold}	T_{hot}	$\delta^*_{corr.}$	$T_{av.}$	$\alpha_T \times 10^3$	$\Omega \times 10^3$
−38.4	−22.8	0.240	−30.8	3.73	15.4
−38.4	−22.8	0.240	−30.8	3.73	15.4
−38.2	−22.9	0.237	−30.7	3.76	15.5
−38.1	−23.0	0.239	−30.7	3.84	15.8
−38.1	−23.0	0.238	−30.7	3.82	15.8
−38.3	−22.7	0.232	−30.7	3.61	14.9
−38.2	−22.8	0.230	−30.7	3.62	14.9
−38.2	−22.8	0.232	−30.7	3.65	15.1
−37.9	−23.0	0.233	−30.6	3.79	15.6

N2-III: big cell/N_2/early data

T_{cold}	T_{hot}	$\delta^*_{corr.}$	$T_{av.}$	$\alpha_T \times 10^3$	$\Omega \times 10^3$
−35.4	−19.7	0.232	−27.7	3.63	14.8
−35.2	−19.5	0.235	−27.5	3.67	15.0

N2-IV: big cell/50 torr N_2/recent data

T_{cold}	T_{hot}	$\delta^*_{corr.}$	$T_{av.}$	$\alpha_T \times 10^3$	$\Omega \times 10^3$
−38.1	−23.1	0.217	−30.8	3.51	14.5
−38.0	−23.2	0.219	−30.8	3.59	14.8
−37.9	−23.1	0.226	−30.7	3.70	15.3
−40.4	−20.3	0.306	−30.6	3.69	15.2
−37.8	−23.1	0.227	−30.6	3.75	15.4
−37.7	−23.2	0.226	−30.6	3.78	15.6
−37.7	−23.2	0.220	−30.6	3.68	15.2
−37.7	−23.2	0.226	−30.6	3.78	15.6
−37.7	−23.1	0.226	−30.5	3.76	15.5
−40.2	−20.3	0.298	−30.5	3.63	15.0
−37.7	−23.0	0.230	−30.5	3.80	15.6

Group	$\langle\delta^*_{blank}\rangle$[b]	N
	−0.005 ± 0.004	5
	−0.001 ± N/A	1
AIR-I	−0.008 ± 0.008	14
	−0.014 ± 0.007	8
	−0.017 ± 0.021	2
	−0.009 ± 0.002	3
	0.005 ± 0.004	12
AIR-II	0.007 ± 0.001	9
	0.006 ± 0.003	9

(continued)

Table 1a. (Continued)

Group	$\langle\delta^*_{blank}\rangle$[b]	N
AIR-III	0.005 ± 0.009	9
AIR-IV	0.007 ± 0.007	8
	0.002 ± 0.010	9
AIR-V	0.002 ± 0.006	16
	0.006 ± 0.002	9
AIR-VI	0.011 ± 0.004	9
N2-I	−0.012 ± N/A	1
	-0.014 ± 0.010	4
N2-II	0.006 ± 0.002	9
N2-III	0.008 ± N/A	1
N2-IV	0.007 ± 0.005	11

[a] Units:
T_{cold}, T_{hot}, $T_{av.}$: °C
$\delta^*_{corr.}$, $\langle\delta^*_{blank}\rangle$: per mil.
Ω ("thermal diffusion sensitivity"): per mil/°C.
α_T ("thermal diffusion factor"): none.
[b] Shown is the average and the standard deviation for a group of blank experiments. The values shown were used to make the background correction for an appropriate set of thermal diffusion experiments using Eqn. 11. *N* is the number of blank experiments used to calculate the average.

2.1.2. Relaxation times for the cells

Thermal diffusion proceeds nominally at the speed of ordinary diffusion, and the composition approaches steady state exponentially (Chapman and Dootson, 1917; Lonsdale and Mason, 1957; Saxena and Mason, 1959; Mason et al., 1966)

$$X_t - X_0 = (X_\infty - X_0)(1 - \exp(-t/\tau)). \quad (10)$$

Here X is the mole fraction of a component of a mixture in either the hot or cold bulb of the equilibration vessel (Fig. 2) at the initial time (denoted by *0*), at some particular time of interest t, or in the steady state (denoted by ∞). The relaxation time is denoted as τ. The amount of time required for the initially uniform composition to reach ~99% of the steady-state value is $\sim 4.5\tau$.

The relaxation times for the cells were found by equilibrating them for various intervals of time and plotting the resulting fractionation as a function of time. We found relaxation times for the big cell and the small cell of ~90 min and ~5 min respectively at 1 atm. In the case of the big cell at 50 torr the relaxation time was reduced to ~6 min (due to the inverse proportionality of the ordinary diffusion coefficient to pressure, see Grew and Ibbs, 1952). The average amount of time allowed for equilibration in our experiments was ~1.5 h for the small cell at 1 atm, ~1 h for the big cell at 50 torr, ~8 h for the early experiments with the big cell at 1 atm, and ~10 h for the recent experiments with the big cell at 1 atm. Thus in all cases we exceeded 5τ.

2.1.3. Gas mixtures used for experiments

Three mixtures were used in our experiments: dry air, H_2O-saturated air, and N_2 (a mixture in the sense that it naturally contains three isotopic species: $^{30}N_2$, $^{29}N_2$, and $^{28}N_2$). Dry air was obtained by pumping the ground level air in La Jolla, California (or Narragansett, Rhode Island for the earliest experiments) into aluminum tanks via a water trap. This was done on days when meteorological conditions were such that pollution of the ambient air was small. Water-saturated air was obtained from the headspace of a 2-L glass flask with deionized water equilibrated with tank dry air (1 atm) at room temperature. Commercial tank nitrogen (N_2) that was used was of ultra-high purity grade (>99.995% N_2).

Table 1b. Summary of the thermal diffusion results for air at −30°C.

Group	$\Omega \times 10^3$, per mil/°C[a]	N	Comment
AIR-I	14.8 ± 0.5	7	small cell/air/early data
AIR-II	14.8 ± 0.5	21	small cell/air/recent data
AIR-III	14.9 ± 0.4	9	small cell/air+vapor/recent data
AIR-IV	14.0 ± 0.8	6	big cell/air/early data (excluded[b])
AIR-V	14.6 ± 0.6	20	big cell/50 torr air/recent data
AIR-VI	14.5 ± 0.2	9	big cell/air/recent data
	14.7 ± 0.5	66	(overall average)[c]

[a] The values were obtained by averaging the results from Table 1a in the vicinity of −30°C after they have been corrected slightly for the temperature offset as described in Section 3. The uncertainty corresponds to the standard deviation 1σ. N is the number of experiments used to calculate the average.

[b] Results were biased and were not included in calculating the overall average (see explanation in Section 4).

[c] Compare with our average result for pure N_2 at −30.6°C: $\Omega = (15.3 \pm 0.4) \times 10^3$ per mil/°C ($N = 20$).

2.1.4. The uniform temperature and dual-temperature baths

A rectangular plastic basin (~35 cm × 23 cm × 11 cm) was used for the blank experiments. It contained water at uniform temperature as a thermal medium. The cells were mounted in it horizontally rather than vertically (because convection was of no concern in this case) using clamps.

The latest version of our dual-temperature bath was made of 3/8″ Plexiglas and had average dimensions roughly 30 cm × 30 cm × 14 cm (Fig. 2, label 2). We attempted to minimize its volume while providing enough space for all the accessories to be inserted. It is worthwhile to mention that the actual bath differed from the drawing in that there was a rectangular volume in its lower left hand part between the bottom and the partition that was separated out and was not a part of the lower section. The associated reduction of volume helped conserve bath fluid and permitted better mixing. The curved shape of the bath at the upper right-hand side was such that both inner valves could be closed off quickly and with minimal perturbation to the temperature in the bath using a specially designed tool. The tool was shaped like a screwdriver and had two pins at its tip matching two small holes drilled on the inner valve handles.

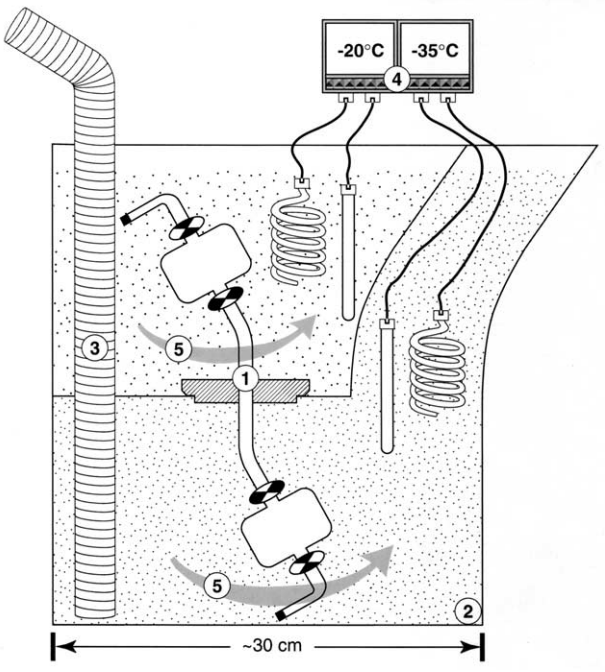

Fig. 2. The setup used in our thermal diffusion experiments. The cell with gas (1) is placed into a bath (2) whose two sections are maintained at two different temperatures. The bath fluid temperatures are brought to their set values by a combined action of a chiller equipped with a probe (3) and the heaters attached to the PID temperature controller (4). The controller is equipped with a pair of temperature sensors and maintains the temperatures at their set values with high precision. The bath fluid is vigorously mixed (5) by a pair of stirrers having long shafts with propellers at their ends. At the termination of the equilibration, the inner valves on the cell are closed off quickly using a specially designed tool. The amount of induced fractionation between the "hot" and "cold" sample volumes is subsequently measured on a mass spectrometer.

Communication of the bath fluid between the two sections was stopped once a cell was inserted into the bath, because the rectangular opening in the partition between the two sections was closed off tightly with a Plexiglas lid permanently attached to a cell (see Fig. 2). Another opening in the partition between sections allowed the chiller probe to penetrate through and tightly fit (see Fig. 2). During equilibrations both the uniform temperature and the dual-temperature baths were placed into thermal insulation boxes of matching dimensions made of 3/4″ gypsum wallboard and fiberglass insulation designed to minimize heat exchange with the room and flammability (the top portion of the thermal diffusion bath remained exposed to air).

2.1.5. Temperature control

The laboratory in which the uniform temperature bath was kept was maintained at a roughly constant temperature of ~21.5°C (±0.3°C). Small fluctuations of air temperature in the room were not noticeable in the water-filled bath as a result of the high heat capacity of water. Of particular concern was the spatial uniformity of temperature in the bath. The latter was determined to be extremely uniform with or without mixing.

Ethyl alcohol was used as a bath fluid in the case of the dual-temperature bath. In a typical experiment, the temperature in the upper section of the bath was set ~15°C higher than in the lower section. A chiller and two heaters were used to drive the temperatures to their set values and to keep them steady afterwards. We found that the best temperature control is achieved when the rate of cooling is maintained constant and varying portions of heat are added to the bath by two small 200-Watt heaters. Hence we always had the chiller in the "on" regime, and the two heaters were constantly switched between "on" and "off" positions by a PID temperature control unit (OMEGA Temperature Handbook). It proved crucial to stir the medium in both sections extremely vigorously to maintain precise and spatially uniform temperature control. Two adjustable speed "propeller" mixers (500 to 10,000 rotations per minute) were used for that purpose.

Temperatures in the two sections were monitored independently from the reading on the temperature control unit by a pair of mercury thermometers (individually calibrated Fisher Scientific total immersion certified thermometers with scale divisions of 0.1°C). The temporal variation of temperature that we typically observed in each section of the bath for the overall duration of an experiment was in the overall range of ±0.2°C or less from the set values. No local differences were

detected by moving a mercury thermometer inside a section as long as the stirring intensity remained appropriate. In recent experiments the temperature of the stainless steel surfaces on the cold and warm sides of a cell were also monitored by attaching to them thermistors connected to high-precision Newport Electronics INFCH-series temperature units. Mercury thermometer temperature readings for the medium in the bath agreed with these surface temperatures, the amplitudes of fluctuations of the latter being somewhat damped because of the metal's thermal inertia.

2.1.6. Experimental procedure

Two alternative procedures were employed for filling the cells with a desired gas as follows.

a) All valves on a cell were opened and it was connected to either tank nitrogen or tank dry air. Flow through a cell was maintained for ~10 min (regulator set to 3 p.s.i.g.). Then the valve on the regulator and the cell's outer upstream and downstream valves were closed off in that order. During the gas flow the downstream end of a cell was connected to a long piece of Decabon tubing which prevented room air from back diffusing into the cell. Most blank samples from the early experiments were not equilibrated in an isothermal bath but rather were analyzed immediately after filling. Because of vigorous flow through the cell, it is unlikely that isotopic fractionation occurred.

b) A cell was connected to a vacuum line on its "warm" end and all the valves on it were opened, except the outer valve on the cold side. A tank with dry air, nitrogen, or the flask containing H_2O-saturated air in the headspace was connected to an adjacent port on the line. The cell and connection to the tank (flask) were evacuated to below 6×10^{-4} torr. For the 1 atm or 50 torr dry gas experiments, a desired amount of gas was metered into a cell by using an intermediate valve (until the capacitance manometer gauge read the desired pressure of 760 or 50 torr). For H_2O-saturated air experiments, air from a flask was expanded directly into the small cell (both were connected to the vacuum line outlets). In that case the resulting pressure in the cell was only slightly less than atmospheric, because the volume of the headspace was ~100 times larger than the sample volume of the cell.

A filled cell had its two outer valves closed and its two inner valves open. The ends of a cell were sealed off (using plastic caps and Parafilm-M plastic film) to prevent bath fluid from entering the tubes, and the cell was mounted in the bath. In the case of a blank experiment, the time count began directly after a cell was placed into the bath (see Section 2.1.2). For a thermal diffusion experiment, the time count began after the temperatures had stabilized at their set values. Temperatures were monitored throughout a thermal diffusion experiment, and their values were documented for the final 10 min with 30 s spacing as read by a pair of mercury thermometers or INFCH readouts (see Section 2.1.5). The average values of the resulting 21 temperature measurements for each section were calculated (a typical standard deviation was <0.1°C), and were later used for calculating the thermal diffusion constants (see Section 3). The experiment was terminated by closing off the inner valves. A cell was then removed from the bath, dried, and brought to a uniform room temperature.

2.1.7. Mass spectrometric analysis

A dual-inlet Finnigan MAT 252 mass spectrometer was used for the isotopic analysis. Generally, "warm" sample was introduced into the bellows on the sample side, and the "cold" sample into the standard side bellows of the mass spectrometer. In the case of water-saturated samples, vapor had to be removed before the analysis. This was achieved by a quantitative transfer of samples via a cold trap (at –100°C) into ~10 cm^3 ~80 cm-long 1/4″ OD stainless steel tubes placed in liquid helium (refer to the experimental technique of Sowers et al., 1989). The samples from the tubes were then introduced to the mass spectrometer. In the case of the big cell at 1 atm, intermediate ~1 cm^3 pipettes were connected to the mass spectrometer's inlet system. Gas from a cell was allowed to equilibrate with the pipettes first, and subsequently the gas from the pipettes was expanded into the bellows. This was done to reduce the gas to an amount the mass spectrometer can accept. In the recent experiments the big cell together with the pipettes were placed into an isothermal water bath (while being connected to the mass spectrometer) to eliminate the possibility of thermal fractionation occurring between the bulbs and the pipettes.

After transferring dry samples into the mass spectrometer, the volume of the bellows was first adjusted roughly such that the pressure was ~38 mbar, and then more precisely manually to ensure an exact balance between the sample and standard ion currents. The isotopic ratio of $^{29}N_2$ to $^{28}N_2$ of gas that was in the hot side of the cell during equilibration relative to that from the cold side was determined 24 times for the early experiments and 144 times for the recent experiments. Note that although measuring "hot" gas vs. "cold" gas actually yields the negative of δ^* (see Eqns. 3, 5, and 6), we always report the absolute values $|\delta^*|$ (Table 1). An automatic Dixon-2 statistical test with 80% confidence level (or more conservative Dixon-3 with 90% confidence level in case of the recent experiments) rejected any outliers (which occurred rarely). Average "delta" values in units of per mil and the corresponding standard deviations were reported by the mass spectrometer's software as a final result.

2.2. Adsorption Fractionation Experiments

A hypothesis can be proposed, that when the molecular nitrogen adsorbed on the surfaces of snow in the firn is desorbed as the firn warms up, a change in firn air isotopic composition will occur. It is possible that the heavier species adsorbs preferentially and makes the firn air isotopically heavier upon desorption. We performed a series of experiments (to which we refer as the "adsorption fractionation experiments") to test this hypothesis. A "snow chamber apparatus" was designed for the experiments (Fig. 3). The cylindrical body of the chamber (Fig. 3, label 1) had two detachable flanges on either side, and the outlets on both flanges were equipped with valves. A piece of firn of cylindrical shape was inserted inside the chamber. Two detachable ~1 cm^3 pipettes (Fig. 3, labels 4 and 5) were connected to the body of the chamber in the middle to allow "sampling" of the firn air.

The first step of the experiment was to introduce clean dry air into the chamber (filled with firn) maintained at –50°C by sustaining a flow of prechilled air through the chamber for 10 min (regulator set to ~3 p.s.i.g.). The air in the chamber (at ~1 atm) was then isolated from the outside by closing Nupro valves V-1 and V-2 on the flanges (Fig. 3). Enough time was allowed for the air composition to become uniform throughout the firn and inside the pipettes (>30 min). Then a sample of air was taken by closing off one of the pipettes (Fig. 3, label V-R). The chamber was then warmed to –15°C and once again enough time was allowed for the air to homogenize isotopically at this new temperature. This "warm" air was sampled by closing off the second pipette (Fig. 3, label V-L). The isotopic composition of the "−50°C" and "−15°C" samples was compared with the aid of the mass spectrometer. If the "desorption fractionation hypothesis" (see above) were correct, then the warm sample would contain a larger fraction of the heavier isotopic species ($^{29}N_2$) than the sample collected before the warming.

Shallow firn from the top portion of a Greenland Dye-3 ice core (from interval ~0–20 m depth) was used for the experiments. An insulated plastic bath (~35 cm × 23 cm × 11 cm) with vigorously mixed ethanol was used as a temperature bath (see Fig. 3). Temperature control was achieved in a fashion similar to the thermal diffusion experiments. "Blank" experiments were performed that attempted to mimic as closely as possible the treatment experiments. Three types of blanks accompanied the experiments as follows: 1) samples were taken from an empty chamber at a constant –50°C, 1 h apart from each other ("simple blank"); 2) samples were taken from an empty chamber before and after warming ("real blank"); 3) samples were taken from the chamber filled with firn at a constant –50°C, the second sample 1 h after the first one ("firn blank").

Samples of air from the pipettes were transferred into the tubes (see Section 2.1.7) via a cold trap maintained at ca. –100°C to remove water vapor. The mass spectrometric analysis of air in the tubes was performed in a similar fashion as in case of thermal diffusion experiments. Twenty-four determinations of the "delta" values for the 29/28 N_2 ratios were obtained on each pair of samples. In contrast to most of the thermal diffusion experiments, a correction to the "delta" values of ca. 0.010 per mil for CO^+ isobaric interference and O_2/N_2 chemical slope was made (Sowers et al., 1989; Severinghaus et al., 1996; Severinghaus et al., 2001).

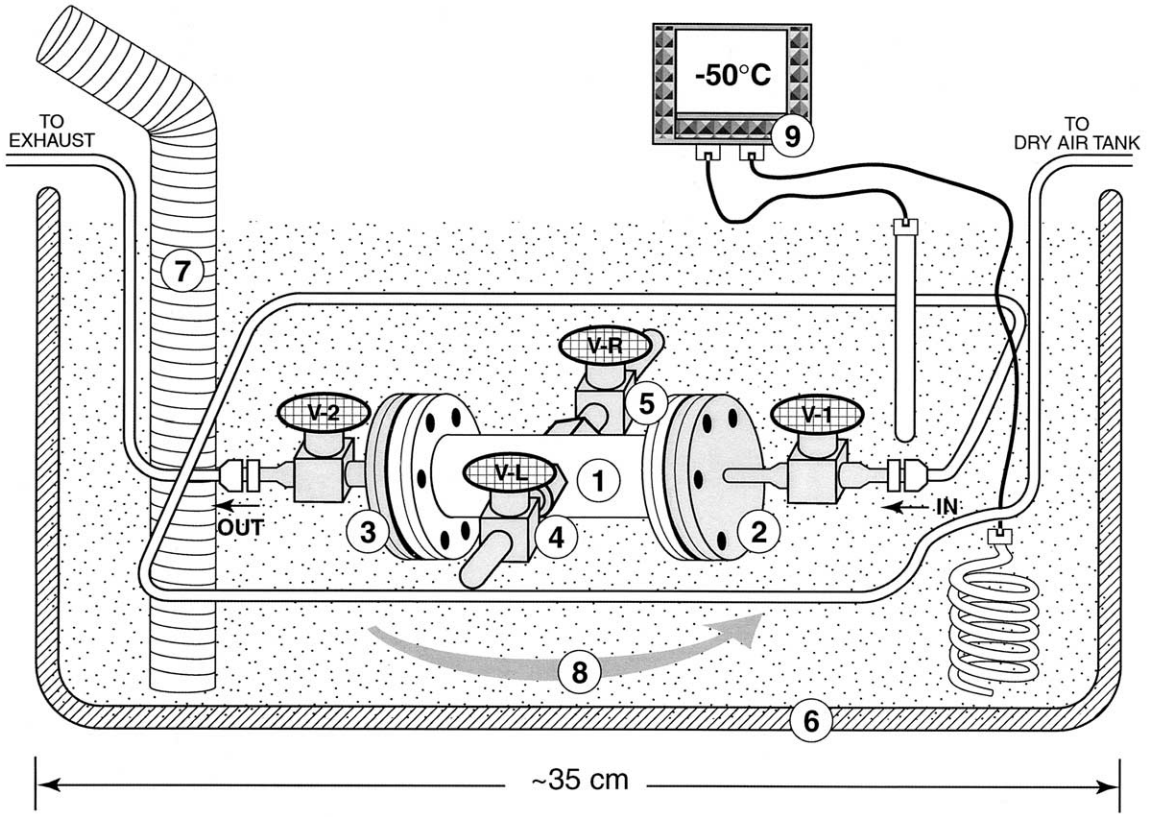

Fig. 3. The setup used in the adsorbtion fractionation experiments. A cylindrical piece of snow firn is inserted into the chamber (1), which is equipped with two detachable flanges (2) and (3). After the air in the chamber has been replaced with the clean, dry (prechilled) air from the tank, valves V-1 and V-2 are closed off. Pipettes (4) and (5) equipped with valves V-L and V-R allow "sampling" of the air inside the chamber once it has been homogenized by diffusion. The bath (6) filled with ethanol serves to keep the apparatus at a desired temperature. The temperature control is achieved in the same fashion as for the thermal diffusion experiments: (7) is the chiller probe, (9) is the temperature controller, while (8) signifies vigorous mixing. The controller maintains the temperature at the set value (−50°C or −15°C). After a sample of air was taken at −50°C, the controller is reset to −15°C and another sample is taken upon equilibration at this new temperature. The pipettes (4) and (5) are then detached and the relative fractionation between them is measured on the mass spectrometer.

3. RESULTS

Results of our thermal diffusion experiments with air and N_2 are shown in Table 1a. Results are subdivided into 10 groups based on what cell and what gas were used for the experiments and whether the experiments were performed before or after we felt that we mastered the experimental technique. Three directly measured parameters are reported for each experiment: the temperatures maintained in the two sections of the bath T_{cold} and T_{hot}, and the amount of fractionation induced by thermal diffusion after reaching the steady state δ^*. To account for a slight drift in the mass spectrometer over time and to obtain a control, blank experiments were routinely performed in between the thermal diffusion experiments (see Section 2.1). Results of the blank experiments expressed as δ^*_{blank} were averaged over periods of time during which the performance of the mass spectrometer was stable and uninterrupted (by a major power outage, for example). These average values $<\delta^*_{blank}>$ (see Table 1a) were then used to make a background correction to the results of the thermal diffusion experiments performed during the same time periods according to the equation:

$$\delta^*_{corr.} = \delta^* - \langle\delta^*_{blank}\rangle. \quad (11)$$

The values of the temperature-dependent thermal diffusion constants α_T and Ω for each experiment were obtained by substituting the values of $\delta^*_{corr.}$, T_{cold}, and T_{hot} into Eqns. 8 and 7 respectively. The effective average temperature of the experiment $T_{av.}$ to which the values of the thermal diffusion constants were referenced was calculated using Eqn. 4. Note that $T_{av.}$ is effectively a proxy for the temperature T on which both constants depend, but which has to be approximated because a finite temperature difference has to be employed to obtain a thermal diffusion signal. The smaller the temperature difference ($T_{hot} - T_{cold}$), the closer is the match between $T_{av.}$ and T. The latter two parameters are often used interchangeably in the literature.

The estimation of errors in the values of α_T and Ω in Table 1a by the propagation of errors calculation is straightforward. Taking the typical values of the parameters that enter in the calculation as $T_{cold} = 238.0 \pm 0.1$ K, $T_{hot} = 253.0 \pm 0.1$ K, and $\delta^*_{corr.} = 0.220 \pm 0.009$ per mil, where the errors correspond to $\sim 1\sigma$, the following result is obtained: $\alpha_T = (3.60 \pm 0.15)$

$\times 10^{-3}$, and $\Omega = (14.7 \pm 0.6) \times 10^{-3}$ per mil/°C. In both cases the error constitutes ~4%. The error in $\delta^*_{corr.}$ that was used here is a combination of a typical error in our mass spectrometric measurements of ~0.005 per mil and the typical error in the average results of blank experiments of ~0.007 per mil. We should point out that the errors in the averages of a series of any experimental values that we report hereafter are the raw standard deviations of the sample and were not divided by the square root of the number of values that were averaged, which makes the errors that we report greater than they would be if the textbook definitions were used. We cannot rule out the presence of small systematic errors on the order of measurement precision in our experiments until our results are confirmed by an independent study. Therefore the errors that we display are indicative of what we feel are more realistic experimental uncertainties at this time.

Most of our thermal diffusion results correspond to an effective average temperature of roughly –30°C. Before the results for air in the vicinity of –30°C (66 datapoints) can be averaged within each group of experiments, they all have to be scaled to a single temperature. This is done by finding the slope of the tangent to the curve that best approximates the temperature dependence of the thermal diffusion sensitivity of $^{29}N_2/^{28}N_2$ in air at –30°C, which is $\sim 0.025 \times 10^{-3}$ per mil/°C increase in Ω per 1°C increase in temperature (see below). The summary of the results for air that correspond to temperatures from –27.5 to –30.9°C scaled to –30°C is shown in Table 1b. The group of results *AIR-IV* is excluded from further consideration as we believe its results were systematically biased as outlined in Section 4. The group *AIR-VI* contains the newer version of the same experiments with the source of bias eliminated.

The errors for the average values of thermal diffusion sensitivity shown in Table 1b are based on a direct calculation from the scatter of datapoints, and are in close agreement with the error in Ω estimated above. The relatively low value of the directly calculated error for group *AIR-VI* is probably fortuitous and does not necessarily represent the realistic error in the results of the blank experiments that entered into the calculation of Ω for this group. With the exception of the results of group *AIR-IV* (excluded), the results of the different groups are not statistically different ($p = 0.95$) from each other within our current estimations of the realistic experimental uncertainties. Hence all the results can be averaged together to obtain the "best" value of the thermal diffusion sensitivity at –30°C, which is $(14.7 \pm 0.5) \times 10^{-3}$ per mil/°C.

The thermal diffusion sensitivity Ω is much less dependent on temperature than the thermal diffusion factor α_T. Hence a single value of Ω of 14.7×10^{-3} per mil/°C could relatively safely be used for the purposes of paleoreconstructions over the whole range of temperatures experienced by the polar environments. On the other hand, knowing the exact value of parameter Ω for each given temperature from that range would further improve the accuracy of the fossil–air paleothermometer. We approach deduction of the empirical equation describing Ω in air as a function of temperature as follows. It was pointed out earlier (see Section 1.2) that a widely used approximation for the temperature dependence of the thermal diffusion factor is given as $\alpha_T \approx a - b/T_K$. This equation implies that the experimental thermal diffusion factors plotted against the reciprocal temperature should fall along a straight line, which is demonstrated for our data for air in Fig. 4. The pooled standard deviation (see below) of all the datapoints relative to the fitted line is $\sim 0.1 \times 10^{-3}$, which agrees well with the magnitude of our experimental uncertainty. Hence we believe it is justified to use the least-squares regression equation

$$\alpha_T \times 10^3 = 8.656 - 1232/T_K \qquad (12)$$

to describe the temperature trend of our results for the thermal diffusion factor of $^{29}N_2/^{28}N_2$ in air. It is understood that T_K here represents the effective average temperature $T_{av.}$.

Having obtained Eqn. 12 allows us to write down a similar equation for the thermal diffusion sensitivity by utilizing the link between α_T and Ω given by Eqn. 9:

$$\Omega = 8.656/T_K - 1232/T_K^2, \text{ per mil/°C.} \qquad (13)$$

Fig. 5 shows the data for air expressed in terms of the thermal diffusion sensitivity plotted against temperature. The curve in Fig. 5 represents Eqn. 13. As a measure of how well the curve represents the data, we calculated the pooled standard deviation of all the datapoints relative to the curve (also termed "goodness of fit"), which is given as the square root of the sum of squared differences between a datapoint and the curve value at the same temperature divided by the number of degrees of freedom. The fact that the pooled standard deviation yielded the value equal to 0.5×10^{-3} per mil/°C in agreement with our experimental uncertainty leads us to conclude that Eqn. 13 is an adequate empirical representation of the temperature dependence of Ω in air as suggested by our results.

At −30°C the value of Ω yielded by Eqn. 13 is 14.8×10^{-3} per mil/°C rather than a "better" value of 14.7×10^{-3} per mil/°C (see above), which, although insignificant, may be kept in mind when the value at −30°C needs to be used for a paleoreconstruction. Based on Eqn. 13 the values of the thermal diffusion sensitivity change as follows: 13.5 at –60°C, 14.5 at –40°C, 15.0 at –20°C, and 15.2×10^{-3} per mil/°C at 0°C. The inset of Fig. 5 shows that the predicted change in Ω based on Eqn. 13 is very nearly linear over the range –32 to –27°C. Therefore the procedure of scaling the datapoints in the vicinity of –30°C to that exact temperature by using a linear slope equal to the temperature derivative to Eqn. 13 at –30°C is justified.

Table 2 displays the results of the supplementary work on "adsorption fractionation" described in this paper (see Section 2.2). The essence of this set of experiments was comparing the isotopic composition of the interstitial firn air before and after a warming of a specially constructed chamber from –50 to –15°C. Results indicate that there is no significant difference in the relative composition compared to zero and also compared to the various blank experiments that were performed.

4. DISCUSSION

In this section we first make three comments regarding our results and then proceed with comparing our thermal diffusion results for N_2 with the data available in the literature. First, it is encouraging that the error in the parameter Ω estimated from the known typical uncertainties in the experimental parameters that enter in its calculation matches the error in the thermal diffusion sensitivity directly calculated from the scatter of results at –30°C. This suggests that unknown sources of ran-

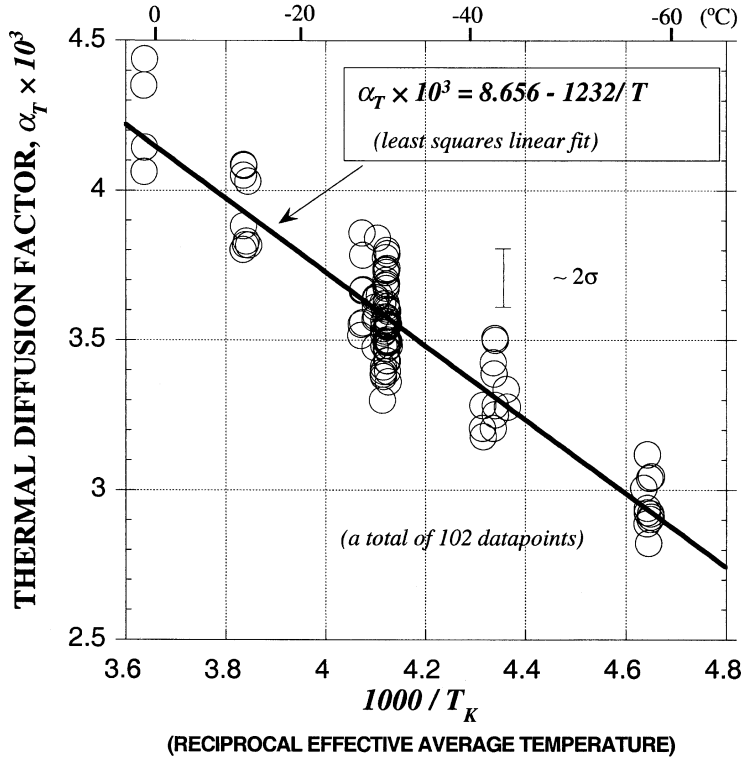

Fig. 4. Thermal diffusion factor α_T for $^{29}N_2/^{28}N_2$ in air obtained from our experiments plotted as a function of $1/T_K$, where T_K is the effective average temperature of an experiment. The datapoints are expected to fall along a straight line on such plot, based on the approximate relation of α_T to temperature $\alpha_T \approx a - b/T_K$.

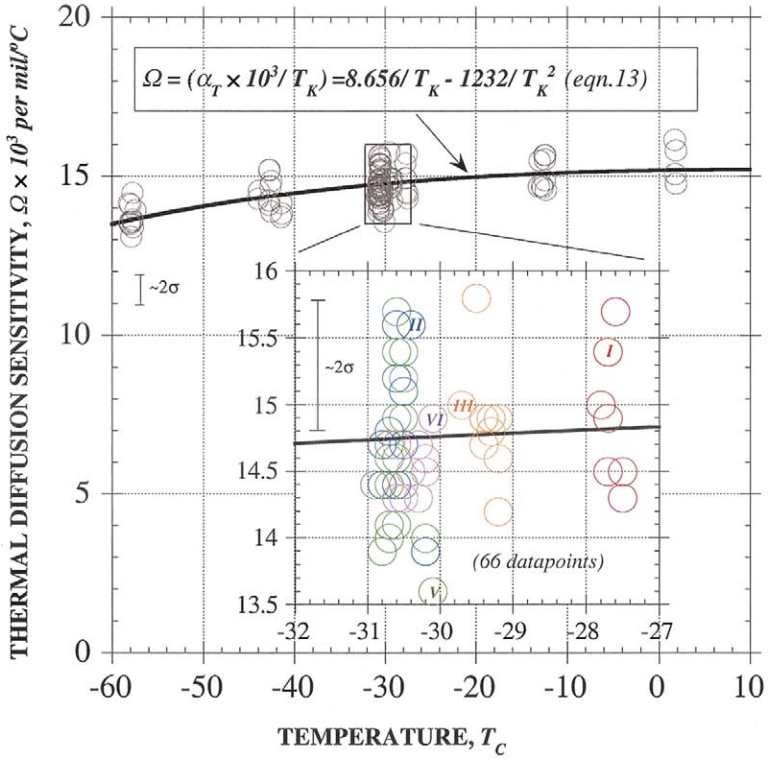

Fig. 5. Thermal diffusion sensitivity Ω for air plotted as a function of temperature (in °C). The curve is not a fit to the data, but rather corresponds to Eqn. 13 which was obtained from the fit of Fig. 4. The inset shows in detail the temperature region where most experiments have been performed. The color and numbers in the inset are used to represent various groups of experiments (namely *AIR-I, II, III, V,* and *VI*).

Table 2. Summary of the adsorption fractionation experiments.

Type of experiment	δ^*, per mil[b]
"Simple blank[a]	0.002
(empty chamber at −50°C, no warming)	0.003
	+0.003 ± 0.001[c]
"Real blank"	−0.014
(empty chamber at −50°C, warming to −15°C)	0.005
	−0.009
	−0.006 ± 0.010
"Firn blank"	0.001
(chamber with firn at −50°C, no warming)	0.003
	+0.002 ± 0.001
Actual experiment	0.015
(chamber with firn at −50°C, warming to −15°C)	−0.007
	0.004
	0.003
	0.000
	−0.007
	−0.004
	−0.019
	−0.003
	−0.002 ± 0.009

[a] See Section 2.2 for a description of the procedures employed for blank experiments and for the actual adsorption fractionation experiments.

[b] The "delta" value corresponds to the analysis of air sampled before the warming (pipette *5*, sample side) versus that sampled after the warming (pipette *4*, standard side).

[c] Shown are average and the standard deviation of a set of results (see Fig. 3).

dom error are not present in our experiments at our current precision level.

Second, it should be mentioned that before obtaining the results of group *AIR-VI* we were puzzled with the significant difference ($p = 0.95$) between the results for group *AIR-IV* (big cell/1 atm air) and the groups *AIR-II* (small cell/1 atm air) and *AIR-V* (big cell/50 torr air), which yielded Ω values of 14.0, 14.6, and 14.8×10^{-3} per mil/°C respectively (results of the group *AIR-III* were not yet available). We thought that a combination of surface effects and of the pressure dependence of thermal diffusion may have caused the offset of $\sim 0.7 \times 10^{-3}$ per mil/°C. Experiments at 50 torr were performed because we wanted to speed up the equilibration time for the big cell. Our principal literature source on thermal diffusion states that there is no effect of pressure on thermal diffusion at low gas densities (Mason et al., 1966), although further reading suggested that this may not always be true (Oost et al., 1972; Dunlop and Bignell, 1996).

As we discovered later by repeating the experiments with greater caution (group *AIR-VI*), experiments of the group *AIR-IV* were biased inadvertently. There was an intermediate sample transfer step in the case of the big cell at 1 atm, which was absent from any other experiments, the purpose of which was to reduce the excessive sample size that the big cell supplies. The procedure involved transferring the two samples from the big cell into 1 cm^3 pipettes. It turns out that if no precaution is made to make the system isothermal during the transfer such that thermal diffusion does not take place between the bulbs of the cell and the pipettes, a bias into the samples may be introduced. Indeed, when care was used to maintain the system in strictly isothermal conditions during the experiments of the group *AIR-VI*, the results turned out essentially the same as the ones for the other groups of experiments. Having found the reason for the offset, we felt justified to reject the results of group *AIR-IV* from any further consideration, while still displaying them in Table 1 for completeness.

Finally, we have long been concerned whether possible temperature-dependent surface adsorption isotopic effects on the stainless steel surfaces may somehow bias the thermal diffusion results. The fact that the results for the big cell and the small cell turn out essentially the same indicates that such effects, if present, are insignificant at our current precision level. Another piece of evidence comes from the moist air results on the small cell. Water molecules may be effective in taking up some of the surface adsorption spaces. Despite this, there is no significant difference between the moist-air results and the results of the other sets of experiments.

At the time when the conflicting results of group *AIR-IV* were obtained, our concerns about the surface effects became particularly strong in view of the fact that snow (firn) has extensive surfaces of adsorption (Domine et al., 2001). If there was an effect on the $^{29}N_2/^{28}N_2$ pair, it would make our "dry-air" thermal diffusion calibration of the fossil paleothermometer to some degree inadequate for the natural polar environment of primary interest to us. This prompted us to carry out a separate set of "adsorption fractionation" experiments aimed at investigating this issue. As was already pointed out, we see no adsorption fractionation effects even though the temperature change in our experiments (−50 to –15°C) was greatly exaggerated compared with the magnitudes of changes experienced by the polar environments during the recent geologic past.

With all the information available to us today, we are led to conclude that while surface effects could induce very small fractionations for $^{29}N_2/^{28}N_2$ in response to temperature changes in laboratory experiments or in nature, it is beyond our current resolution level to detect them. As later reading revealed, Trengove et al. (1981) were confronted with concerns similar to ours with regard to their thermal diffusion experiments on mixtures of helium with other gases. They resolved the issue by placing a copper cleaning pad in one of the bulbs of their thermal diffusion apparatus (which increased its surface area by a factor of ~2) and saw no difference in the results with or without the pad within the experimental uncertainty.

We now turn to the data on thermal diffusion of isotopic nitrogen in pure gas that was recovered from the literature (Table 3). Note that in some cases thermal diffusion of the $^{30}N_2/^{28}N_2$ isotopic pair was studied rather than the $^{29}N_2/^{28}N_2$ pair, but fortunately there is a well-established relationship that allows one to convert the results between different isotopic species of the same gas with great accuracy (Saxena and Mason, 1958). Another point worth mentioning is that the study of Boersma-Klein and de Vries (1966) was originally intended for the "slope" method of deducing the thermal diffusion factor (Mason et al., 1966) instead of the more conventional way by employing Eqn. 3. However the authors failed to carry out all the steps needed to deduce the α_T values from their raw data. They fitted their data for the parameter q (see Eqn. 5) with a curve derived from their thermal diffusion experiments on isotopic CO and mislabeled the curves so that to an unsuspect-

Table 3. Literature data for the isotopic thermal diffusion factor of N_2.[a]

$T_{av.}$[b]	reference (1[c])
103.4	−1.69 ± 0.05
118.2	−0.65 ± 0.42
130.1	0.57 ± 0.09
231.0	3.70 ± 0.72
363.3	5.89 ± 0.72
408.8	5.63 ± 0.51
504.8	6.35 ± 0.56
603.2	6.23 ± 0.42
677.5	6.37 ± 0.91
736.1	6.11 ± 0.79

$T_{av.}$	reference 2*	reference (2†)
142.5	1.47	1.36
143.7	1.49	1.42
144.8	1.50	1.48
160.5	1.72	
168.4	2.09	1.89
168.4	1.97	
172.2	2.16	1.83
173.1	2.06	1.73
173.1	2.18	1.85
178.7	2.17	
187.5	2.24	2.21
190.1	2.44	2.12
190.1	2.59	2.27
198.5	2.52	2.40
226.7	3.38	
236.4	3.67	3.73
241.1	3.69	3.61
245.7	3.70	3.45
247.7	3.20	3.26
251.5	3.80	4.39
258.9	4.08	
269.1	3.75	4.37
271.9	4.71	
279.9	4.78	
280.4	4.90	5.40
281.0	5.86	5.11

$T_{av.}$	reference (3)
433.7	9.10 ± 0.40
435.1	8.90 ± 0.90
281.3	7.10 ± 0.50
281.6	7.80 ± 1.20

$T_{av.}$	reference (4)
329.7	5.10 ± 0.51

[a] The data were obtained from the following references: 1) Raman et al. (1968); 2) Boersma-Klein and de Vries (1966):

* 29/28 N_2 experiments,

† 30/28 N_2 experiments; 3) Davenport and Winter (1951); 4) Mann (1948). In order to convert all of the data to a single format, the data from ref. 1 were divided by a factor of 57, and the data from ref. 2† were multiplied by a factor of 29/57 in accordance with the law of proportionality of the isotopic thermal diffusion factor to $(M_1 - M_2)/(M_1 + M_2)$, where M_i are the masses of the isotopic molecules in consideration (see Mason et al., 1966).

[b] Effective average temperature (in Kelvin)

[c] $\alpha T \times 10^3$ obtained from the listed reference

ing reader it appears that the fit (for which they listed an equation) is in fact a very good one. Although we did reanalyze their data using the slope method, we refrain from using it in this paper because the results are highly sensitive to the form of the α_T temperature dependence assumed, and the original data are too noisy for the procedure to be carried out with confidence. On the other hand, calculation of the thermal diffusion factors through the use of Eqn. 3, while undermining the possibility of an "exact" (in theory) assignment of the thermal diffusion factors to temperature, permits viewing their data before the scatter has been artificially removed.

Figure 6 shows the literature data plotted in terms of the thermal diffusion factor against the effective average temperature $T_{av.}$. We chose to omit the data of Davenport and Winter (1951) from the plot as they appear biased towards higher values. The origin of this bias is unclear. We included our two average datapoints for pure N_2: $\alpha_T = (3.71 \pm 0.09) \times 10^{-3}$ at 242.5 K and $\alpha_T = (3.66 \pm 0.08) \times 10^{-3}$ at 245.5 K in Fig. 6 (refer to Table 1a). We did not attempt to "scale" our results for N_2 to the temperature of –30.0°C as we did in Table 1b for air, because in the case of pure N_2 we do not know the temperature trend of the thermal diffusion factor with high precision. It may be noted that our error bars (2σ) are the size of the symbols in Figure 6 and amount to less than 0.2×10^{-3}, whereas the typical literature error bars in Fig. 6 are a factor of five larger.

The inset of Figure 6 shows clearly that our data support the previously available data within their range of uncertainty while establishing the magnitude of the α_T value with unmatched precision at the effective average temperature of roughly −30°C. The same procedure as in Figure 4 was performed to obtain the following empirical equation representing all of the data for N_2 shown in Figure 6:

$$\alpha_T \times 10^3 = 7.980 - 1003/T_K. \quad (14)$$

Unlike Eqn. 12 this equation, while applicable over a very broad range of temperatures, allows only a crude estimation of α_T at various temperatures because of the fitted data being sparse and mostly characterized by a large uncertainty. The data such as that contained in Figure 6 for isotopic nitrogen can serve as a powerful testground for intermolecular potential models (Saxena and Mathur, 1966; Maitland et al., 1981).

5. CONCLUSIONS

A new experimental setup allowing fractionation of gas mixtures in a known temperature difference by thermal diffusion in the laboratory has been described. Unlike techniques used by previous workers, the experimental procedure is fast and less laborious. Small temperature differences are used in our procedure. This gives an advantage of more accurate assignment of the acquired thermal diffusion constants to the average temperature, but requires very sensitive equipment to be able to detect the fractionation with high precision. The disadvantage of our method is that it can only be applied over a relatively narrow temperature range (ca. −60 to 0°C). We performed 108 thermal diffusion experiments using air as a study mixture and 30 experiments using pure N_2 as a study mixture. This allowed us to determine the precise values of the thermal diffusion constants for the $^{29}N_2/^{28}N_2$ isotopic pair in air and in N_2. Our results for N_2 support the previously available literature data and constrain the absolute value of the

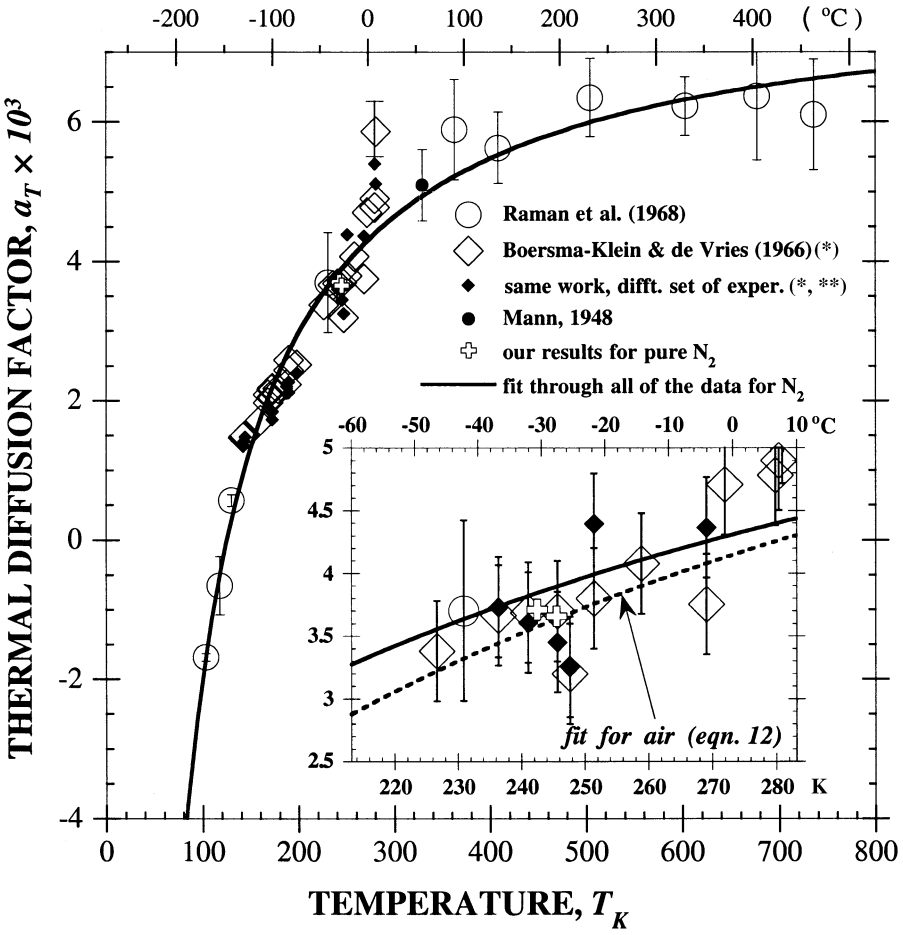

Fig. 6. Literature data for the thermal diffusion factor of $^{29}N_2/^{28}N_2$ in pure N_2 plotted as a function of temperature (see Table 3). Our two averaged results are shown for comparison. The solid curve is an unweighted fit to all of the pure N_2 data (including ours) of the form $\alpha_T = a - b/T_K$. Shown for comparison in the inset is the dashed curve representing our data for air (Eqn. 12). (*) Typical experimental error of Boersma-Klein and de Vries (1966) was estimated from their statement that a typical measurement error in q (Eqn. 5) was 0.2% while taking into account that their trennschaukel had 8 tubes. No account was taken of the errors in the reported temperatures, since the authors did not indicate them. (A typical error bar for that work is shown in conjunction with one datapoint only in order to preserve the clarity of the figure.) (**) Data based on the $^{30}N_2/^{28}N_2$ experiments of Boersma-Klein and DeVries (1966), see Table 3.

thermal diffusion factor at –30°C with an uncertainty a factor of five smaller than the previously available data.

The thermal diffusion constants of $^{29}N_2/^{28}N_2$ in air were determined for the first time and are shown to be slightly less than the results in N_2, as may be anticipated due to the modifying effect of the "third" major gas (oxygen) in air (see Fig. 6). Whereas the thermal diffusion constants for N_2 were only determined at a single temperature of ca. –30°C in our experiments, the constants for air covered a range of temperatures from ca. −60 to 0°C, which allowed us to deduce the slight trend of the thermal diffusion sensitivity with temperature in this case. It should be emphasized that the trend with the temperature is a second-order feature. Of foremost importance is the absolute value of the thermal diffusion sensitivity at a selected temperature, which we find to be $(14.7 \pm 0.5) \times 10^{-3}$ per mil/°C at −30°C. To account for the slight temperature variation of the thermal diffusion sensitivity, the following empirical equation may be used to find its value at any temperature of interest in the range −60 to 0°C: Ω ($^{29}N_2/^{28}N_2$, air) $= 8.656/T_K - 1232/T_K^2$ (±ca. 3%) per mil/°C.

In addition, a separate experimental setup was used to investigate whether temperature change–induced fractionation of the polar firn air can also result (in addition to the thermal diffusion process) from differing affinities of isotopic molecules for adsorption on the snow surfaces at different temperatures. Our "adsorption fractionation" experiments for $^{29}N_2/^{28}N_2$ in air have essentially eliminated that possibility, at least at the current resolution level.

Acknowledgments—We wish to express our gratitude to Prof. Michael Bender for hosting us in his laboratory in the University of Rhode Island where some of our first thermal diffusion experiments were performed in 1997–98. We thank many colleagues who shared their helpful comments and suggestions regarding this work, especially at its early stages, most notably Profs. Michael Bender, Devendra Lal, Richard Alley, Ray Weiss, Ralph Keeling, and Andrew Dickson. The two anonymous reviewers and the associate editor (Dr. David Cole) sup-

plied very valuable criticisms that helped to improve the original version of the manuscript. We are greatly indebted to the pioneers of thermal diffusion studies for paving the road to this work. This study was supported by NSF grants (to J.P.S.) ATM99-05241, OPP97-25305, and the Scripps Institution of Oceanography Director's office.

Associate editor: D. Cole

REFERENCES

Alley R. B., Anandakrishnan S., Jung P., and Clough A. (2001) Stochastic resonance in the North Atlantic: Further insights. In *The Oceans and Rapid Climate Change: Past, Present, and Future* (eds. D. Seidov, B. J. Haupt, and M. Maslin), pp. 57–68. AGU, Washington, DC.

Blunier T. and Brook E. J. (2001) Timing of millennial-scale climate change in Antarctica and Greenland during the Last Glacial Period. *Science* **291,** 109–112.

Boersma-Klein V. and De Vries A. E. (1966) The influence of the distribution of atomic masses within the molecule on thermal diffusion, I: Isotopic CO and N_2 molecules. *Physica* **32,** 717–733.

Boushehri A., Bzowski J., and Mason E. A. (1987) Equilibrium and transport properties of eleven polyatomic gases at low density. *J. Phys. Chem. Ref. Data* **16,** 449–466.

Brown H. (1940) On the temperature assignments of experimental thermal diffusion coefficients. *Phys. Rev.* **58,** 661–662.

Bzowski J., Kestin J., Mason E. A., and Uribe F. J. (1990) Equilibrium and transport properties of gas mixtures at low density: Eleven polyatomic and five noble gases. *J. Phys. Chem. Ref. Data* **19**(5), 1179–1232.

Caillon N., Jouzel J., and Chappellaz J. (2001) Reconstruction of the surface temperature change in Central Greenland during D/O 12, 45 Kyr B.P. *Eos (Transactions, AGU)* **82**(47), p. F23 (abstr.).

Chapman S. (1917) The kinetic theory of simple and composite monatomic gases: Viscosity thermal conduction, and diffusion. Reprinted in: Brush, S. G. (1972). *Kinetic Theory*, Vol. 3, p. 102 Pergamon, New York.

Chapman S. and Dootson F. W. (1917) A note on thermal diffusion. *Phil. Mag.* **33,** 248–253.

Chapman S. and Cowling T. G. (1970) *The Mathematical Theory of Non-Uniform Gases: An Account of the Kinetic Theory of Viscosity, Thermal Conduction and Diffusion in Gases*. Cambridge Univ. Press, Cambridge, 422 p.

Cowling T. G. (1970) Approximate theories of thermal diffusion. *J. Phys.* **3A,** 774–782.

Davenport A. N. and Winter E. R. S. (1951) Diffusion properties of gases: Part V. The thermal diffusion of carbon monoxide, nitrogen and methane. *Trans. Faraday Soc.* **47,** 1160–1169.

De Groot S. R. (1959) *Thermodynamics of Irreversible Processes*. North-Holland, Amsterdam.

Domine F., Cabanes A., Taillandier A. S., and Legagneux L. (2001) Specific surface area of snow samples determined by CH_4 adsorbtion at 77 K and estimated by optical microscopy and scanning electron microscopy. *Environ. Sci. Technol.* **35,** 771–780.

Dunlop P. J. and Bignell C. M. (1996) Pressure dependencies of the thermal diffusion factors, of nine helium-fluoroethane systems at 300 K: Prediction of the variation with temperature of the limiting diffusion coefficients of these systems from α_T values at zero pressure. *J. Chem. Phys.* **104**(1), 1–4.

Enskog D. (1917) Kinetic theory of processes in dilute gases. Reprinted in: Brush S. G. (1972) *Kinetic Theory*, Vol. 3. p. 125 Pergamon, New York. .

Frankel S. P. (1940) Elementary derivation of thermal diffusion. *Phys. Rev.* **57**(7), 661.

Furry W. H. (1948) On the elementary explanation of diffusion phenomena in gases. *Am. J. Phys.* **16**(2), 63–78.

Grew K. E. and Ibbs T. L. (1952) *Thermal Diffusion in Gases*. Cambridge Univ. Press, New York. 143 p.

Grew K. E. (1969) Thermal diffusion. In *Transport Phenomena in Fluids* (ed. H. J. M. Hanley), pp. 333–376. Dekker, New York.

Hirschfelder J. O., Curtiss C. F., and Bird R. B. (1964) *Molecular Theory of Gases and Liquids*. Wiley, New York. 1249 p.

Jones R. C. and Furry W. H. (1946) The separation of isotopes by thermal diffusion. *Rev. Mod. Phys.* **18**(2), 151–224.

Jouzel J. (1999) Calibrating the isotopic paleothermometer. *Science* **286,** 910–911.

Kestin J., Knierim K., Mason E. A., Najafi B., Ro S. T., and Waldman M. (1984) Equilibrium and transport properties of the noble gases and their mixtures at low density. *J. Phys. Chem. Ref. Data* **13**(1), 229–303.

Kincaid J. M., Cohen E. G. D., and Lopez de Haro M. (1987) The Enskog theory for multicomponent mixtures. IV. Thermal diffusion. *J. Chem. Phys.* **86**(2), 963–975.

Lang C., Leuenberger M., Schwander J., and Johnsen S. (1999) 16°C rapid temperature variation in Central Greenland 70,000 years ago. *Science* **286,** 934–937.

Leuenberger M. C., Lang C., and Schwander J. (1999) Delta(15)N measurements as a calibration tool for the paleothermometer and gas-ice age differences: A case study for the 8200 BP event on GRIP ice. *J. Geophys Res.* **104**(D18), 22163–22170.

Lonsdale H. K. and Mason E. A. (1957) Thermal diffusion and the approach to the steady state in H_2-CO_2 and He-CO_2. *J. Phys. Chem.* **61,** 1544–1551.

Maitland G. C., Rigby M., Smith E. B., and Wakeham W. A. (1981) *Intermolecular Forces: Their Origin and Determination*. Clarendon Press, New York. 616 p.

Mann A. K. (1948) The thermal diffusion constant of nitrogen. *Phys. Rev.* **73,** 412–413.

Mason E. A., Munn R. J., and Smith F. J. (1966) Thermal diffusion in gases. *Adv. At. Mol. Phys.* **2,** 33–91.

Monchick L. and Mason E. A. (1967) Free-flight theory of gas mixtures. *Phys. Fluids* **10**(7), 1377–1390.

Moran T. I. and Watson W. W. (1958) Thermal diffusion factors for the noble gases. *Phys. Rev.* **109**(4), 1184–1190.

Oost W. A. (1968) On the pressure dependence of the thermal diffusion factor for binary mixtures up to 80 atmospheres. Ph.D. thesis, Leiden, 100 p.

Oost W. A., Los J., Cauwenbergh H., and Van Dael W. (1972) Thermal diffusion in moderately dense gas mixtures and the pair-correlation function. *Physica* **62,** 409–426.

Paul R., Howard A. J., and Watson W. W. (1963) Isotopic thermal diffusion factor for argon. *J. Chem. Phys.* **39**(11), 3053–3056.

Present R. D. (1958) *Kinetic Theory of Gases*. McGraw-Hill, New York. 280 p.

Raman S., Mathur B. P., Howard A. J., Champlin J. W., and Watson W. W. (1968) Thermal diffusion in polyatomic gases: Isotopic $^{15}N_2$-$^{14}N_2$. *J. Chem. Phys.* **49,** 4877–4879.

Rutherford W. M. (1973) Isotopic thermal diffusion factors for Ne, Ar, Kr, and Xe from column measurements. *J. Chem. Phys.* **58**(4), 1613–1618.

Santamaria C. M., Saviron J. M., and Yarza J. C. (1977) Isotopic thermal diffusion factors of the noble gases. *Physica* **89A,** 90–96.

Saxena S. C. and Mason E. A. (1958) Higher approximations for the transport properties of binary gas mixtures: III. Isotopic thermal diffusion. *J. Chem. Phys.* **28**(4), 623–625.

Saxena S. C. and Mason E. A. (1959) Diffusion coefficients of gases from the rate of approach to the steady state in thermal diffusion. *Mol. Phys.* **2,** 264–270.

Saxena S. C., Kelley J. G., and Watson W. W. (1961) Temperature dependence of the thermal diffusion factor for helium, neon and argon. *Phys. Fluids* **4**(10), 1216–1225.

Saxena S. C. and Mathur B. P. (1966) Thermal diffusion in isotopic gas mixtures and intermolecular forces. *Rev. Mod. Phys.* **38**(2), 380–390.

Severinghaus J. P., Bender M. L., Keeling R. F., and Broecker W. S. (1996) Fractionation of soil gases by diffusion of water vapor, gravitational settling, and thermal diffusion. *Geochim. Cosmochim. Acta* **60,** 1005–1018.

Severinghaus J. P., Sowers T., Brook E. J., Alley R. B., and Bender M. L. (1998) Timing of abrupt climate change at the end of the Younger Dryas interval from thermally fractionated gases in polar ice. *Nature* **391,** 141–146.

Severinghaus J. P. and Brook E. J. (1999) Abrupt climate change at the end of the last glacial period inferred from trapped air in polar ice. *Science* **286,** 930–934.

Severinghaus J. P., Grachev A. M., Battle M. (2001). Thermal fractionation of air in polar firn by seasonal temperature gradients. *Geochem. Geophys. Geosyst.* **2**, paper #2000GC000146.

Severinghaus J. P., Grachev A., Luz B., and Caillon N. (2003) A method for precise measurement of argon 40/36 and krypton/argon ratios in trapped air in polar ice with applications to past firn thickness and abrupt climate change in Greenland and at Siple Dome, Antarctica. *Geochim. Cosmochim. Acta* **67**(3).

Sowers T., Bender M., and Raynaud D. (1989) Elemental and isotopic composition of occluded O_2 and N_2 in polar ice. *J. Geophys. Res.* **94**(D4), 5137–5150.

Stevens G. A. and de Vries A. E. (1968) The influence of the distribution of atomic masses within the molecule on thermal diffusion. II. Isotopic methane and methane/argon mixtures. *Physica* **39,** 346–360.

Stier L. G. (1942) The coefficients of thermal diffusion of neon and argon and their variation with temperature. *Phys. Rev.* **62,** 548–551.

Taylor W. L. and Weissman S. (1973) Isotopic thermal diffusion factors for argon and krypton. *J. Chem. Phys.* **59**(3), 1190–1195.

Trengove R. D., Robjohns H. L., Martin M. L., and Dunlop P. J. (1981) The pressure dependences of the thermal diffusion factors of the systems He-Ar, He-CO_2, and He-SF_6 at 300 K. *Physica* **108A,** 502–510.

Van der Valk F. and De Vries A. E. (1963) Thermal diffusion in ternary mixtures, II: Experiments. *Physica* **29,** 427–436.

Velds C. A., Los J., and De Vries A. E. (1967) Thermal diffusion at moderate pressures in He-CO_2 mixtures. *Physica* **35,** 417–440.

APPENDIX

The relationship between α_T ($T_{av.}$) and Ω ($T_{av.}$) can be derived as follows. We start with the expression for α_T of Eqn. 8 and notice the following:

1) If $0.001 \times \delta^* \ll 1$, then $\ln (1 + 0.001 \times \delta^*) \approx 0.001 \times \delta^*$ (using Taylor expansion to the first order);

2) Definition of $T_{av.}$ (Eqn. 4) can be rewritten as $\ln (T_{hot}/T_{cold}) = \Delta T \times T_{av.}/(T_{hot} \times T_{cold})$, where $\Delta T \equiv T_{hot} - T_{cold}$;

3) The latter expression can be transformed by noticing that if T_{hot} and T_{cold} are close to each other, then
$T_{hot} \times T_{cold} \approx T_{av.}^2$; hence $\ln (T_{hot}/T_{cold}) \approx \Delta T/T_{av.}$.

Equation 8 can now be approximated as
$\alpha_T (T_{av.}) \approx (\delta^*/\Delta T) \times 0.001\ T_{av.}$. By observing that the expression in the parenthesis is the definition of Ω ($T_{av.}$) (Eqn. 7), we arrive at the final simple equation relating the thermal diffusion sensitivity Ω ($T_{av.}$) to the thermal diffusion factor α_T ($T_{av.}$):
$\Omega (T_{av.}) = \alpha_T (T_{av.}) \times 1000/T_{av.}$, where the units of $T_{av.}$ are degrees Kelvin and the units of Ω are per mil/°C.